Image Reconstruction of Buried Inhomogeneous Dielectric Cylinders Coated on a Conductor

Chun Jen Lin, Chien-Ching Chiu

Electrical Engineering Department, Tamkang University, Taipei, Republic of China

ABSTRACT: The image reconstruction of buried inhomogeneous dielectric cylinders coated on a conductor with known cross-section is investigated. Inhomogeneous dielectric cylinders coated on a conductor is buried in one half space and scatter a group of unrelated waves incident from another half space, where the scattered field is recorded. By proper arrangement of the various unrelated incident fields, the difficulties of ill-posedness and nonlinearity are circumvented, and the permittivity distribution can be reconstructed through simple matrix operations. The algorithm is based on the moment method and the unrelated illumination method. Numerical results show that good reconstruction has been obtained both with and without Gaussian noise in measured data.   © 2005 Wiley Periodicals, Inc. Int J Imaging Syst Technol, 15, 172–177, 2005; Published online in Wiley InterScience (www.interscience.wiley.com). DOI 10.1002/ima.20049

I. INTRODUCTION

Electromagnetic inverse scattering problems of underground objects have been a growing importance in many different fields of applied science, with a large potential impact on geosciences and remote sensing applications (Chiu and Kiang, 1991; Caorsi et al., 1992; Chiu and Huang, 1996; Tsihrintzis et al., 1999; Akhtar and Omar, 2000; Cui and Chew, 2000, 2002; Miller et al., 2000; Bucci et al., 2001; Meincke, 2001; Rekanos and Tsiboukis, 2002; Leone and Soldovieri, 2003; Rekanos and Raisanen, 2003). Typical examples are the detection of buried electric cord, power and communication cables, archaeological remains and so on. The solutions are considerably more difficult than those involving objects in free space. This is due to the interaction between the air–earth interface and the object, which leads to the complicated Green's function for this half-space problem. It is well known that one major difficulty of inverse scattering is its ill-posedness nature (Sabatier, 1983). Ill-posedness means that a small error in the measured field data may cause a large error in the reconstructed result. This problem is also ill-posed because of the face that the kernel of the integral is a smoothing function. Ill-posedness may be caused by the natural limitation for propagating waves to carry high spatial frequency information or by the limited ability of the reconstruction algorithm to make efficient use of the measured data. Nonlinearity is another difficulty. The inverse scattering problem is nonlinear in nature because it involves the product of two unknowns, the electrical property of object and the electric field within the object.

In the past few years, several numerical techniques have been reported for electromagnetic imaging reconstruction. Generally speaking, two kinds of approaches have been developed. The first is an approximate approach. It makes use of diffraction tomography type of technique to determine the permittivity of buried dielectric objects (Cui and Chew, 2000, 2002; Meincke, 2001; Leone and Soldovieri, 2003). However, this method requires some approximations, such as Born approximation for buried dielectric objects. In contrast, the second approach is to solve the exact equation of the imaging problem by numerical method (Chiu and Kiang, 1991; Caorsi et al., 1992; Chiu and Huang, 1996; Tsihrintzis et al., 1999; Akhtar and Omar, 2000; Miller et al., 2000; Bucci et al., 2001; Rekanos and Tsiboukis, 2002; Rekanos and Raisanen, 2003). The technique needs no approximation in formulation, but the calculation is more complex when compared with the approximate approach. However, the second approach merely dealt with the case of simple objects, i.e., the scatters are either buried conductors or buried dielectric objects only and there is still no rigorous algorithm for the case involving both conductors and dielectric objects at the same time. A typical example for the aforementioned case is the conductors coated by the buried inhomogeneous dielectric materials.

In this paper, the inverse scattering for buried complex objects, i.e., scatterer involving both conductors and dielectric objects is investigated. An efficient algorithm is proposed to reconstruct the permittivity distribution of the objects by using only the scattered field measured outside. The algorithm is based on the unrelated illumination method (Wang and Zhang, 1992; Chiu, 1996). In Section II, the theoretical formulation for electromagnetic inverse scattering is presented. Numerical results for objects of different permittivity distributions are given in Section III. Finally, conclusions are drawn in Section IV.

II. THEORETICAL FORMULATION

Let us consider inhomogeneous dielectric cylinders with relative permittivity $\varepsilon_r(r)$ coated on a conductor buried in a lossless homo-
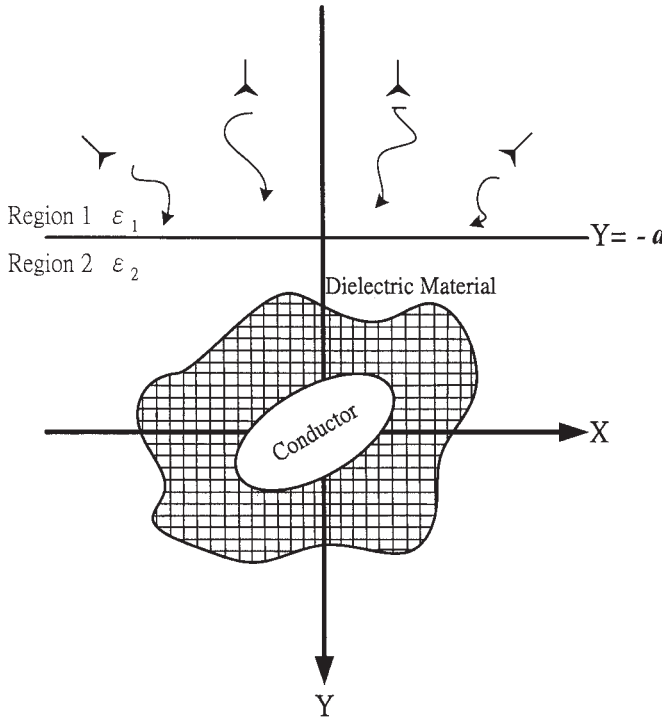

Figure 1. Geometry of problem in the (x, y) plane.

geneous half-space as shown in Figure 1. Media in regions 1 and 2 are characterized by permittivities ε_1 and ε_2, respectively. The permeability is μ_0 for all material, including the scatterers. The axis of the buried cylinders is the z-axis; that is, the properties of the scatterer may vary with the transverse coordinates only. A group of unrelated incident wave with electric field parallel to the z-axis (i.e., transverse magnetic) is illuminated upon the scatterers. Owing to the interface between region 1 and 2, the incident waves generate two waves that would exist in the absence of the scatterer: reflected waves (for $y \leq -a$) and transmitted waves (for $y > -a$). Let the unperturbed field be represented by

$$\bar{E}^i(x, y) = \begin{cases} (E^i)_1(x, y)\hat{z}, & y \leq -a \\ (E^i)_2(x, y)\hat{z}, & y > -a \end{cases}. \tag{1}$$

Then the internal total electric field inside the inhomogeneous dielectric object, $\bar{E}(x, y) = E(x, y)\hat{z}$, can be expressed by the following integral equation

$$E^i(\bar{r}) = \int_s G(\bar{r}, \bar{r}')k_2^2[\varepsilon_r(\bar{r}') - 1]E(\bar{r}')\,ds'$$
$$- j\omega\mu_0 \int_c G(\bar{r}, \bar{r}')J_s(\bar{r}')\,dl' + E(\bar{r}), \quad y > -a \tag{2}$$

with

$$G(x, y; x', y') = \begin{cases} G_1(x, y; x', y'), & y \leq -a \\ G_2(x, y; x', y') = G_f(x, y; x', y') & \\ + G_s(x, y; x', y'), & y > -a, \end{cases} \tag{3a}$$

$$G_1(x, y; x', y') = \frac{1}{2\pi} \int_{-\infty}^{\infty} \frac{j}{\gamma_1 + \gamma_2} e^{j\gamma_1(y+a)} e^{-j\gamma_2(y'+a)} e^{-ja(x-x')}\,d\alpha, \tag{3b}$$

$$G_f(x, y; x', y') = \frac{j}{4}H_0^{(2)}\left(k_2\sqrt{(x-x')^2 + (y-y')^2}\right), \tag{3c}$$

$$G_s(x, y; x', y') = \frac{1}{2\pi} \int_{-\infty}^{\infty} \frac{j}{2\gamma_2}\left(\frac{\gamma_2 - \gamma_1}{\gamma_2 + \gamma_1}\right) e^{-j\gamma_2(y+2a+y')} e^{-ja(x-x')}\,d\alpha, \tag{3d}$$

$$\gamma_i^2 = k_i^2 - \alpha^2, \quad i = 1, 2, \ \text{Im}(\gamma_1) \leq 0, \ y' > -a.$$

Here k_i and ε_r denote the wave number in region i and the relative permittivity of the dielectric objects. J_s is the induced surface current density, which is proportional to normal derivative of the electric field on the conductor surface. $G(x, y; x', y')$ is the Green's function, which can be obtained by the Fourier transform (Chiu and Kiang, 1991). In (3c), $H_0^{(2)}$ is the Hankel function of the second kind of order 0. For numerical implementation of Green's function, we might face some difficulties in calculating this function. This Green's function is in the form of an improper integral, which must be evaluated numerically. However, the integral converges very slowly when (x, y) and (x', y') approach the interface $y = -a$. Fortunately we find that the integral in G_1 or G_2 may be rewritten as a closed-form term plus a rapidly converging integral (Chiu and Kiang, 1991). Thus the whole integral in the Green's function can be calculated efficiently.

The boundary condition states that the total tangential electric field must be zero on the surface of the perfectly conducting cylinder and this yields the following equation

$$\left[E^i(\bar{r}) = \int_s G(\bar{r}, \bar{r}')k_2^2[\varepsilon_r(\bar{r}') - 1]E(\bar{r}')\,ds' \right.$$
$$\left. - j\omega\mu_0 \int_c G(\bar{r}, \bar{r}')J_s(\bar{r}')\,dl'\right]_{\bar{r}\varepsilon c}, \quad y > -a. \tag{4}$$

The scattered field, $\bar{E}^s(x, y) = E^s(x, y)\hat{z}$, can be expressed as

$$E^s(\bar{r}) = -\int_s G(\bar{r}, \bar{r}')k_2^2[\varepsilon_\gamma(\bar{r}') - 1]E(\bar{r}')\,ds'$$
$$+ j\omega\mu_0 \int_c G(\bar{r}, \bar{r}')J_s(\bar{r}')\,dl'. \tag{5}$$

For the direct scattering problem, the scattered field is computed by giving the permittivity distribution of the buried inhomogeneous dielectric cylinders coated on conductor objects. This can be achieved by using (2) and (4) to solve the total field inside the object E and calculating E^s by (5). For numerical implementation of the direct problem, the dielectric objects are divided into N_1 sufficient small cells. Similarly, we divide the contour of the conductor into N_2 sufficient small segments so that the induced electric and equivalent magnetic surface current density can be considered constant over each segment. Thus the permittivity and the total field within each cell can be taken as constants. Then the moment method is used to solve
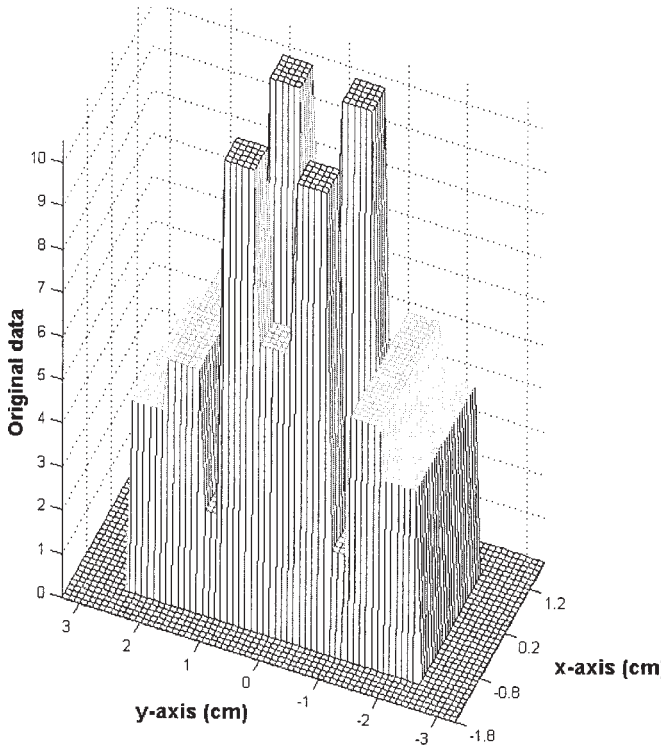
Figure 2. Original relative permittivity distribution for example 1.

(2)–(4) with a pulse basis function for expansion and point matching for testing. Thus the following matrix equations can be obtained:

$$(E^i) = [[G_3][\tau] + [I]](E) + [G_4](J_s), \qquad (6)$$

$$(E_v^i) = [G_5][\tau](E) + [G_6](J_s), \qquad (7)$$

$$(E^s) = -[G_7][\tau](E) + [G_8](J_s), \qquad (8)$$

where (E^i) and (E) represent the N_1 element incident field column vectors. (E_v^i) is the N_2 element incident field column vectors. (E^s) denotes the M-element scattered field column vectors. Here M is the number of measurement points. The matrices $[G_3]$ and $[G_4]$ are $N_1 \times N_1$ and $N_1 \times N_2$ square matrices, respectively. The matrices $[G_5]$ and $[G_6]$ are $N_2 \times N_1$ and $N_2 \times N_2$ matrices. The matrices $[G_7]$ and $[G_8]$ are $M \times N_1$ and $M \times N_2$ matrices. The element in matrices $[G_i]$, $i = 3, 4, 5\ldots 8$ can be obtained by tedious mathematic manipulation (see Appendix). $[\tau]$ is $N_1 \times N_1$ diagonal matrices whose diagonal elements are formed from the permittivities of each cell minus one. $[I]$ is a identity $N_1 \times N_1$ matrix. We can solve the direct problem by using (6)–(8).

We consider the following inverse problem: the permittivity distribution of the inhomogeneous dielectric cylinders coated on conductor objects is to be computed by knowing the scattered field measured in region 1. Note that the only unknown permittivity is ε_r (r). In the inversion procedure, we choose N_1 different incident column vectors. Then Eqs. (6)–(8) can be expressed as

$$[E_p^i] = [[G_{p1}][\tau] + [I]][E], \qquad (9)$$

$$[E_p^s] = -[G_{p2}][\tau][E], \qquad (10)$$

where

$$[E_p^i] = [E^i] - [G_4][G_6]^{-1}[E_v^i],$$

$$[E_p^s] = [E^s] - [G_8][G_6]^{-1}[E_v^i],$$

$$[G_{p1}] = [G_3] - [G_4][G_6]^{-1}[G_5],$$

$$[G_{p2}] = [G_8][G_6]^{-1}[G_5] + [G_7],$$

Here $[E_p^i]$ is a $N_1 \times N_1$ matrix. $[E_p^s]$ is a $M \times N_1$ matrix. Note the matrix $[G_6]$ is diagonally dominant and always invertible. It is worth mentioning that other than the matrix $[G_{p2}]$, the matrix $[G_{p1}][\tau] + [I]$ is always a well-posed one in any case. Therefore, by first solving $[E]$ in (9) and substituting it into (10), then $[\tau]$ can be found by solving the following equations

$$[\Psi][\tau] = [\Phi], \qquad (11)$$

where

$$[\Phi] = -[E_p^s][E_p^i]^{-1},$$

$$[\Psi] = [E_p^s][E_p^i]^{-1}[G_{p1}] + [G_{p2}].$$

From (11), all the diagonal elements in the matrix $[\tau]$ can be determined by comparing the element with the same subscripts, which may be any row of both $[\Psi]$ and $[\Phi]$:

$$(\tau)_{nn} = \frac{(\Phi)_{mn}}{(\Psi)_{mn}}. \qquad (12)$$

Note that there are a total of M possible values for each element of τ. Therefore, the average value of these M data is computed and chosen as final reconstruction result in the simulation.
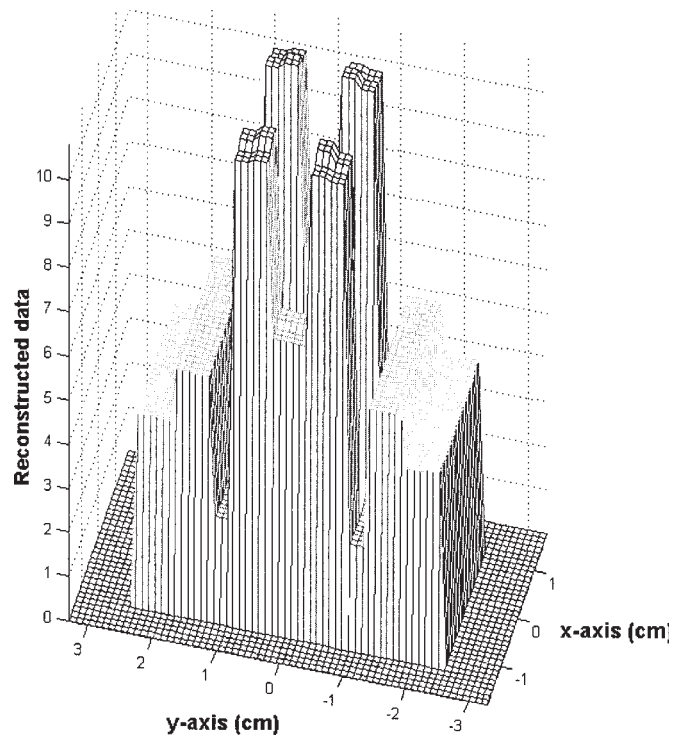

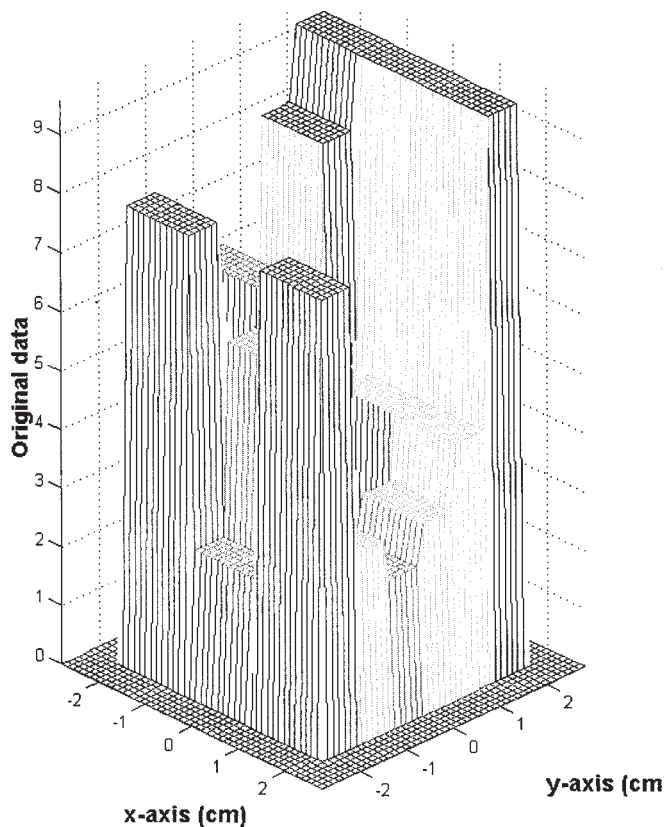**Figure 3.** Reconstructed relative permittivity distribution for example 1.

Figure 4. Original relative permittivity distribution for example 2.

is taken on a half circle of radius 3 m about $(0, -a)$ at equal spacing. The number of measurement point is set to be 8 for each illumination. For avoiding trivial inversion of finite dimensional problems, the discretization number for the direct problem is four times than that for the inverse problem in our numerical simulation.

A 1.2×1.8 cm^2 rectangular cross-section of a perfectly conducting rod coated with buried dielectric materials with rectangular cross-sections is our first example. The buried dielectric material is discretized into 8×16 cells and the corresponding dielectric permittivities are plotted in Figure 2. The model is characterized by simple step distribution of permittivity. Each cell has 0.3×0.3 cm^2 cross-sections. The reconstructed permittivity distributions of the object are plotted in Figure 3. The root-mean-square (RMS) error is about 1.1%. It is clear that the reconstruction is good.

In the second example, the 1.4×1.4 cm^2 square cross-section of a perfectly conducting rod coated with buried dielectric materials with square cross-sections is discretized into 12×12 cells, and the corresponding dielectric permittivities are plotted in Figure 4. Each cell has 0.35×0.35 cm^2 cross-sections. The reconstructed permittivity distributions of the object are plotted in Figure 5. The RMS error is about 1.48%. We can see the reconstruction is also good.

For investigating the effect of noise, we add to each complex scattered field a quantity $b + c_j$, where b and c are independent random numbers having a Gaussian distribution over 0 to the noise level times the rms value of the scattered field. The noise levels applied include 10^{-5}, 10^{-4}, 10^{-3}, 10^{-2}, and 10^{-1} in the simulations. The numerical results for example 1 and 2 are plotted in Figure 6 and Figure 7, respectively. It is seen that the effect of noise is tolerable for noise levels below 1%.
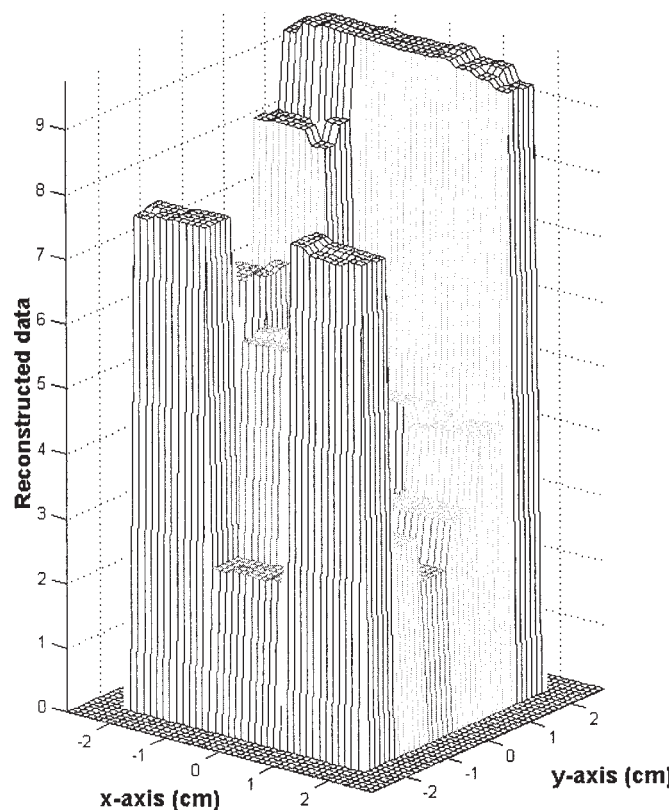
In the above derivation, the key problem is that the incident matrix $[E_p^i]$ must not be a singular matrix, i.e., all the incident column vectors that form the $[E_p^i]$ matrix, must be linearly unrelated. Thus, if the object is illuminated by a group of unrelated incident waves, it is possible to reconstruct the permittivity distribution of the objects. Note that when the number of cells becomes very large; it is difficult to make such a great number of independent measurements. In such a case, some regularization methods must be used to overcome the ill-posedness.

III. NUMERICAL RESULTS

In this section, we report some numerical results obtained by computer simulations using the method described in the Section II. Let us consider an inhomogeneous dielectric cylinder coated on a conductor buried at a depth of $a = 0.1$ m in a lossless half space, as shown in Figure 1. The permittivities in region 1 and 2 are characterized by $\varepsilon_1 = \varepsilon_0$ and $\varepsilon_2 = 2.25\varepsilon_0$. The frequency of the incident waves is chosen to be 3 GHz and the number of illuminations is the same as that of cells. The incident waves are generated by numerous groups of radiators operated simultaneously.

Each group of radiators is restricted to transmit a narrow-bandwidth pattern that can be implemented by antenna array techniques. By changing the beam direction and tuning the phase of each group of radiators, one can focus all the incident beams in turn at each cell of the object. This procedure is named *beam focusing* (Wang and Zhang, 1992). Note that this focusing should be set when the scatterer is absent. Clearly, an incident matrix formed in this way is diagonally dominant and its inverse matrix exists. The measurement

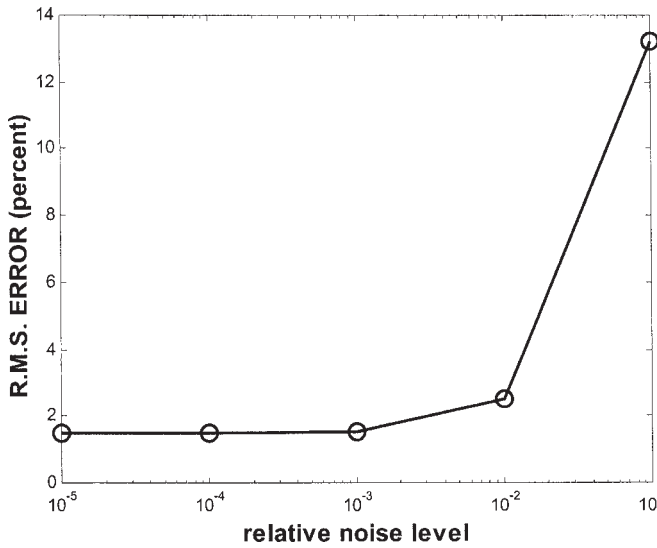**Figure 5.** Reconstructed relative permittivity distribution for example 2.

Figure 6. Reconstructed error as a function of noise level for example 1.

IV. CONCLUSIONS

An efficient algorithm for reconstructing the permittivity distribution of buried inhomogeneous dielectric cylinders coated on a conductor has been proposed. By properly arranging the direction and the polarization of various unrelated waves, the difficulty of ill-posedness and nonlinearity is avoided. Thus, the permittivity distribution can be obtained by simple matrix operations. The moment method has been used to transform a set of integral equations into matrix form. Then these matrix equations are solved by the unrelated illumination method. Numerical simulation for imaging the permittivity distribution of a buried inhomogeneous dielectric cylinders coated on a conductor has been carried out and good reconstruction has been obtained even in the presence of Gaussian noise in measured data. This algorithm is very effective and efficient, since no iteration is required.
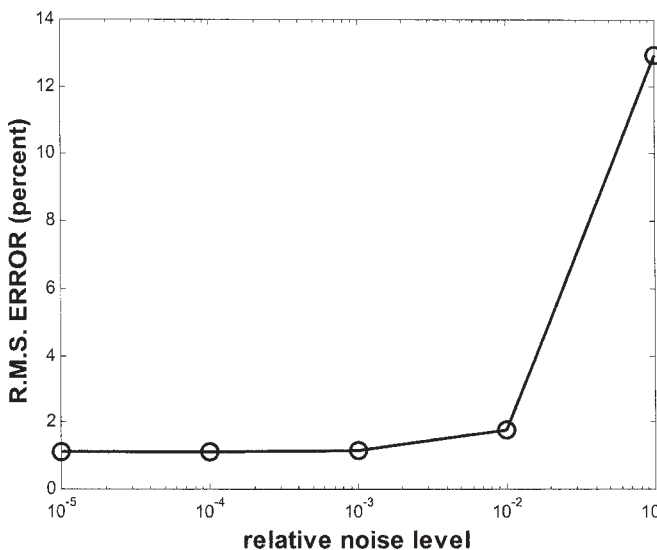

Figure 7. Reconstructed error as a function of noise level for example 2.

APPENDIX

The element in the matrix $[G_1]$ can be written as

$$(G_3)_{mn} = \left[k_2^2 \iint_{\text{cell } n} G_2(x,y;x',y') \, dx' \, dy' \right]_{\substack{x=x_m \\ y=y_m}},$$

where (x_m, y_m) is the observation point located in the center of the mth cell. For a sufficient small cell, we can replace the cell by a circular cell with the same cross-section (Richmond, 1965). Let the equivalent radius of the nth circular cell be a_n. The $(G_3)_{mn}$ can be expressed in the following form

$$(G_3)_{mn} = \begin{cases} G_s(x_m,y_m;x_n,y_n)k_2^2\bar{\Delta}S_n \\ \quad + \frac{j\pi k_2 a_n}{2} J_1(k_2 a_n)H_0^{(2)}(k_2\rho_{mn}), & m \neq n \\ G_s(x_m,y_m;x_n,y_n)k_2^2\bar{\Delta}S_n \\ \quad + \frac{j}{2}[\pi k_2 a_n H_1^{(2)}(K_2 a_n) - 2j], & m = n \end{cases}$$

with $\rho_{mn} = \sqrt{(x_m - x_n)^2 + (y_m - y_n)^2}$, where (x_n, y_n) is the center of the cell n. ΔS_n denotes the area of the nth cell. J_1 is Bessel function of the first order.

The element in the matrix $[G_4]$ can be written as

$$(G_4)_{mn} = \left[-j\omega\mu_0 \int_{\text{segment } n} G_2(x,y;x',y') \, dl' \right]_{\substack{x=x_m \\ y=y_m}},$$

where (x_m, y_m) is the observation point located in the center of the mth cell.

The $(G_4)_{mn}$ can be expressed in the following form

$$(G_4)_{mn} = -j\omega\mu_0[G_f(x_m,y_m;x_n,y_n) + G_s(x_m,y_m;x_n,y_n)]\Delta C_n,$$

where (x_n, y_n) is the center of the cell n. ΔC_n denotes the length of the nth segment on the surface of the perfectly conductor.

Similarly,

$$(G_5)_{mn} = G_s(x_m,y_m;x_n,y_n)k_2^2 \, \Delta S_n + \frac{j\pi k_2 a_n}{2} J_1(k_2 a_n)H_0^{(2)}(k_2\rho_{mn}),$$

$$(G_6)_{mn} = \begin{cases} -j\omega\mu_0 \cdot G_s(x_m,y_m;x_n,y_n) \cdot \Delta C_n \\ \quad + \frac{\omega\mu_0}{4}\Delta C_n H_0^{(2)}(k_2\rho_{mn}), & m \neq n \\ -j\omega\mu_0 \cdot G_s(x_m,y_m;x_n,y_n) \cdot \Delta C_n \\ \quad + \frac{\omega\mu_0}{4}\Delta C_n\left[1 - j\frac{2}{\pi} \ln\frac{\gamma k_2\Delta C_n}{4e}\right], & m = n \end{cases}$$

where $\ln \gamma = 0.5772156649$

$$(G_7)_{mn} = G_1(x_m,y_m;x_n,y_n)k_2^2\Delta S_n,$$

$$(G_8)_{mn} = j\omega\mu_0 \cdot G_1(x_m,y_m;x_n,y_n)\Delta S_n.$$

REFERENCES

M.J. Akhtar and A.S. Omar, Reconstructing permittivity profiles using integral transforms and improved renormalization techniques, IEEE Trans Microw Theo Tech 48 (2000), 1385–1393.

O.M. Bucci, L. Crocco, T. Isernia, and V. Pascazio, Subsurface inverse scattering problems: quantifying, qualifying, and achieving the available information, IEEE Trans Geosci Rem Sens 39 (2001), 2527–2538.

S. Caorsi, G.L. Gragnani, and M. Pastorino, Numerical solution to three-dimensional inverse scattering for dielectric reconstruction purposes, IEE Proc H 139 (1992), 45–52.

C.C. Chiu, Inverse scattering of inhomogeneous biaxial materials coated on a conductor, IEEE Trans Antenn Propag 46 (1996), 218–225.

C.C. Chiu and C.P. Huang, Inverse scattering of dielectric cylinders buried in a half space, Microw Opt Tech Lett 13 (1996), 96–99.

C.C. Chiu and Y.M. Kiang, Inverse scattering of a buried conducting cylinder, Inverse Probl 7 (1991), 187–202.

T.J. Cui and W.C. Chew, Novel diffraction tomographic algorithm for imaging two-dimensional targets buried under a lossy earth, IEEE Trans Geosci Rem Sens 38 (2000), 2033–2041.

T.J. Cui and W.C. Chew, Diffraction tomographic algorithm for the detection of three-dimensional objects buried in a lossy half-space, IEEE Trans Antenn Propag 50 (2002), 42–49.

R.F. Harrington, Field computation by moment methods, Macmillan, New York, 1968.

A. Ishimaru, Electromagnetic wave propagation, radiation and scattering, Prentice-Hall, Englewood Cliffs, NJ, 1991.

G. Leone and F. Soldovieri, Analysis of the distorted born approximation for subsurface reconstruction: Truncation and uncertainties, IEEE Trans Geosci Rem Sens 41 (2003), 66–74.

P. Meincke, Linear GPR inversion for lossy soil and a planar air-soil interface, IEEE Trans Geosci Rem Sens 39 (2001), 2713–2721.

E.L. Miller, M. Kilmer, and C. Rappaport, A new shape-based method for object localization and characterization from scattered field data, IEEE Trans Geosci Rem Sens 38 (2000), 1682–1696.

I.T. Rekanos and A. Raisanen, Microwave imaging in the time domain of buried multiple scatterers by using an FDTD-based optimization technique, IEEE Trans Magn 39 (2003), 1381–1384.

I.T. Rekanos and T.D. Tsiboukis, An inverse scattering technique for microwave imaging of binary objects, IEEE Trans Microw Theo Tech 50 (2002), 1439–1441.

J.H. Richmond, Scattering by a dielectric cylinder of arbitrary cross section shape, IEEE Trans Antenn Propag 13 (1965), 334–341.

P.C. Sabatier, Theoretical considerations for inverse scattering, Radio Sci 18 (1983), 1–18.

G.A. Tsihrintzis, P.M. Johansen, and A.J. Devaney, Buried object detection and location estimation from electromagnetic field measurements, IEEE Trans Antenn Propag 47 (1999), 1742–1744.

W. Wang and S. Zhang, Unrelated illumination method for electromagnetic inverse scattering of inhomogeneous lossy dielectric bodies, IEEE Trans Antenn Propag 40 (1992), 1292–1296.